BBA - Molecular Basis of Disease 1865 (2019) 454–463

Contents lists available at ScienceDirect

BBA - Molecular Basis of Disease

journal homepage: www.elsevier.com/locate/bbadis

MLL3 enhances the transcription of PD-L1 and regulates anti-tumor immunity

Wei Xiong, Huanghao Deng, Changkun Huang, Chong Zen, Chengzhu Jian, Kun Ye, Zhaohui Zhong, Xiaokun Zhao, Liang Zhu*

Department of Urology, The Second Xiangya Hospital, Central South University, Changsha 410011, China

ARTICLE INFO

Keywords:
PD-L1
MLL3
Prostate cancer
Immune evasion

ABSTRACT

Tumor cells utilize the overexpression of the programmed death-1 ligand 1(PD-L1) to escape T-cell controlled immune-surveillance. The clinical therapy that dilapidates PD1 or PD-L1-mediated cancer tolerance has pushed out the need to uncover the molecular regulation of PD-L1 overexpression in the tumor cell. In this study, we identify histone methyltransferase mixed-lineage leukemia protein 3 (MLL3) as a critical regulator of PD-L1 in prostate cancer cells. MLL3 and PD-L1 were highly expressed in the metastatic cancer tissues, compared to the primary cancer tissues. Furthermore, their expressions were highly correlated in the cancer tissues in the databases of TCGA and Xiangya Hospital. We found that MLL3 bound to the enhancer of PD-L1. Depletion of MLL3 decreased the binding level of H3K4me1 in the enhancer of PD-L1 and Pol II Ser-5p in the promoter of PD-L1. Importantly, MLL3 depletion impaired the mouse xenograft growth and decreased the response to PD-L1 antibody treatment in mice. The findings extend the understanding of the biology regulation of PD-L1 transcription and identify the histone writer MLL3 in an important immune checkpoint, and give prominence to a hidden therapeutic target to conquer immune evasion by tumor cells.

1. Introduction

Complicated and differentiated multi-cellular organisms exploit the integrated binding of transcription factors (TFs). These TFs usually bind to distally cis-regulatory elements, also known as enhancers. These events spatiotemporally facilitate exact programs of the gene expression during cancer progression or development [1,2]. In the cancer progression or development, enhancers exhibit stereotypical and complicated patterns in chromatin. These modification and organization of enhancers are difference among cell types and are conserved across the same species [1,3]. These distally cis-regulatory elements are bound by multi-transcription factors and the complexes of coactivators, and are flanked by specific histone modifications. In the enhancer regions, there are the acetylation of histone H3 on lysine 27 (H3K27ac) and monomethylation of histone H3 on lysine 4 (H3K4me1) [4,5].

Although in the cells, the histone modification markers are loyally correlated with the enhancer activity and states, their precise function on enhancer or neighbors' promoter remain unclear. Recently, the enzymes worked for writing the functional enhancer modifications have been found. The MLL/COMPASS family was identified as the histone writer for enhancer. MLL3 (also known as KMT2C) and MLL4 (also known as KMT2D) belong to the MLL/COMPASS family, and have been identified as the major H3K4 mono-methyltransferase for enhancer [6]. The MLL3 and MLL4 are the huge molecular weight proteins, and both of their C-terminals contained SET domains responsible for the H3K4me1 catalysis. Several groups found that both MLL3 and MLL4 associate with some genes' enhancers and facilitate their transcriptions. Furthermore, they recruit other coactivators, like p300, which acetylates at H3K27 [7]. It has been reported that knocking down of MLL3 and MLL4 decreased the activity of enhancer, and the H3K4me1 served as an important histone marker to label the enhancer activity [2,8]. However, the precise regulation of MLL/COMPASS family in the enhancer remains less understand.

In the immune cells, multiple inhibition pathways have been reported to attenuate immune responses. The immune feedback systems mainly are ligand-receptor-binding manners. For example, the antigen-presenting cells (APCs) connect with T cells using the receptors (like programmed death 1 (PD1)) or ligands (like programmed death ligand 1(PD-L1, also known as CD274)) [9]. PD1 is belonging to a family of the CD28/CTLA-4. The interaction between PD1 and PD-L1 triggers an inhibitory signal which inhibits the activated T cells [10–12]. In the cancer cells, this PD1 and PD-L1 signaling inhibits immune response of

* Corresponding author.
E-mail address: zhuliang@csu.edu.cn (L. Zhu).

https://doi.org/10.1016/j.bbadis.2018.10.027
Received 9 May 2018; Received in revised form 13 October 2018; Accepted 26 October 2018
Available online 30 October 2018

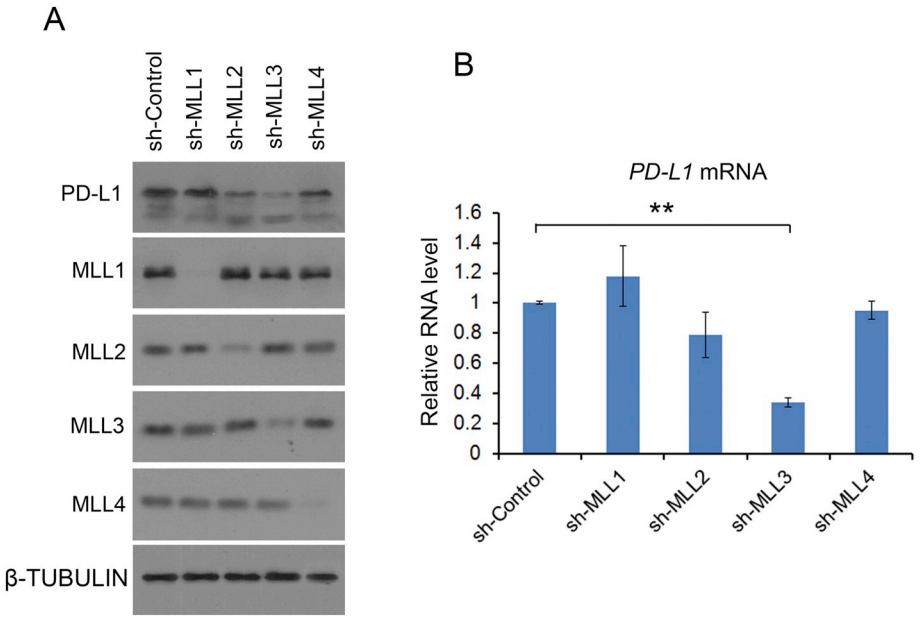

Fig. 1. MLL3 upregulated *PD-L1* expression in the prostate cancer cell.
(A and B) PC-3 cells were infected with lentivirus expressing control or MLL1, MLL2, MLL3 and MLL4-specific shRNAs. 72 h after infection, cells were harvested for WB (A) or RT-qPCR (B). All data are shown as mean values ± SD (n = 3). ns, not significant, $^{**}P < 0.001$ comparing to the control group.

Table 1
The correlation between the expressions of MLL3 and PD-L1 with clinic pathologic features.

Characteristic		MLL3 expression		*P*-value	PD-L1 expression		*P*-value
		High	Low		High	Low	
Age	< 50	7	9	0.134	9	7	0.211
	≥50	25	25		27	23	
Gleason score	≤6	13	8	0.339	11	10	0.199
	> 6	22	23		26	19	
Tumor stage	I + II	10	6	0.037	10	6	0.021
	III + IV	33	17		35	15	
PSA recruitment (30 months) metastasis	No	13	6	0.008	13	6	0.013
	Yes	36	11		35	12	
	No	15	10	0.001	16	9	0.003
	Yes	39	2		35	6	

anti-tumor process [13–15]. There are two types of T-cells, including a subset of $CD4^+CD25^+$ T cells and a subset of $CD8^+CD122^+$ T cells. Both of subsets of T cells play important roles in maintaining self-tolerance and escaping from autoimmunity [16]. Tumor cells expressing PD-L1 evade immune attacks [14,17].

Here, we found that PD-L1 and MLL3 were positively correlated in the cancer tissues of the TCGA database and our database. We also found that MLL3 bound to the enhancer of PD-L1. Depletion of MLL3 decreased the binding of H3K4me1 in the enhancer of PD-L1 and Pol II Ser-5p in the promoter of PD-L1. Importantly, MLL3 depletion impaired mouse xenograft growth and decreased the response to the PD-L1 antibody treatment. The findings enlarge the understanding of the biology regulation of PD-L1 transcription and identify the histone writer MLL3 in the important immune checkpoint, and supply a potential therapeutic target to conquer immune evasion by tumor cells.

2. Results

2.1. MLL3 was a critical regulator of PD-L1 in prostate cancer cells

Increasing evidences suggest that members of the MLL/COMPASS family play important roles in cancer progression, especially in cancer metastasis [2]. Tumors may exploit T-cell inhibitory signals to inhibit the antitumor immune response, thus facilitating immune evasion of the tumor cell. PD-L1 is expressed in tumor cells and is the key factor of immune evasion [14]. To explore the potential regulation of PD-L1 in prostate cancer cells by the MLL/COMPASS family, we used the PC3 human prostate cancer cell line, which has high metastatic ability. MLL1, MLL2, MLL3 and MLL4 were individually knocked down in the PC3 cells. The knocking down efficiency was about 80% for each MLL (Fig. 1A). In the PC3 cells, depletion of MLL3 decreased protein expression of PD-L1 by about 80% and depletion of MLL2 decreased protein expression of PD-L1 by about 40%. Depletion of MLL1 or MLL4 had no effect on PD-L1 protein expression (Fig. 1A). Quantitative reverse transcription polymerase chain reaction (RT-qPCR) results showed that knocking down MLL3, but not the other MLLs, reduced the RNA levels of *PD-L1* (Fig. 1B). These data suggest that MLL3 may be a major transcriptional regulator of PD-L1 in prostate cancer cells.

2.2. MLL3 and PD-L1RNA levels were highly correlated in cancer tissues

To identify the role of MLL3 in the progression of prostate cancer, and to demonstrate the functional and physiological link between MLL3 and PD-L1, 66 metastatic castration-resistant prostate cancer (CRPC) tissue samples were collected for further study; 23 of these samples were paired with primary prostate cancer tissue samples. The RNA levels of *MLL3* and *PD-L1* in the tissues, measured by RT-qPCR, were positively correlated with tumor metastasis and prostate-specific antigen (PSA) recruitment of patients, but not with Gleason scores, patients' ages or tumor stages (Table 1). Furthermore, in the 23 paired CRPC samples, the RNA levels of *MLL3* and *PD-L1* were higher in the metastatic CRPC samples than in the primary prostate cancer samples

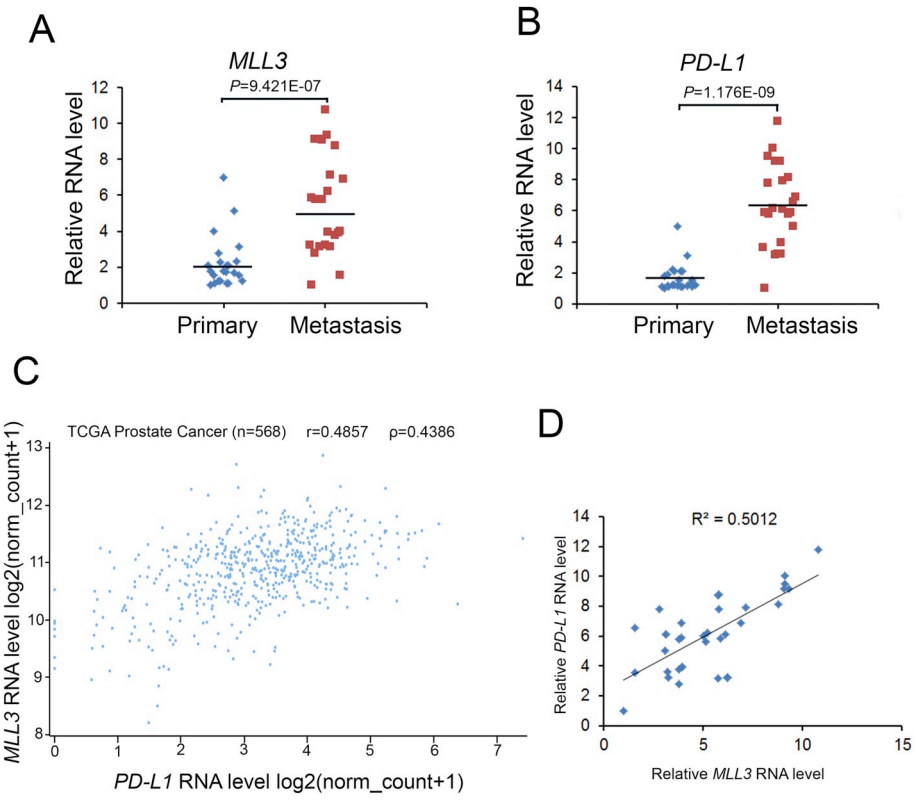

Fig. 2. MLL3 and *PD-L1* expressions had a correlation in prostate cancer tissues.
(A and B) Comparison of CD274 (PD-L1) mRNA (poly(A)) expression and MLL3 mRNA (poly(A)) expression among CRPC patient samples. The patient's samples were frozen and smashed by the hammer. The small tissues were harvested in the Trizol and extracted the RNAs. The Student *t*-test was used for the statistical test.
(C) The correlation of expression of MLL3 and PD-L1 in TCGA database. The correlation analysis was using UCSC XENA online tool (http://xena.ucsc.edu).
(D) The correlation of expression of MLL3 and PD-L1 in Xiangya Hospital database. The patient's samples were frozen and smashed by the hammer. The small tissues were harvested in the Trizol and extracted the RNAs. The Spearman test was used for the statistical test.

(Fig. 2A and B). Importantly, we found that the RNA levels of *PD-L1* were correlated with *MLL3* in The Cancer Genome Atlas (TCGA) database and 35 patients' samples of Xiangya Hospital's (Changsha, China) database. In the Fig. 2D, the relative level of *MLL3* RNA expression was plotted against the relative level of *PD-L1* expression. Statistical analysis showed Spearman correlation coefficients of 0.4857 and 0.5012 ($P < 0.01$) between the TCGA database and 35 patients' samples of Xiangya Hospital's database (Fig. 2D). These data revealed a significant correlation between the RNA levels of MLL3 and PD-L1 expression in the clinical specimens.

2.3. MLL3 regulated the enhancer activity of PD-L1

It has been reported that MLL3 regulates H3K4 mono-methylation (H3K4me1) in the enhancer regions. Notably, H3K4me1 is a mark for the enhancer region and H3k4me3 is a marker for the promoter. We determined the promoter region and potential enhancer region of PD-L1 through the published histone ChIP-seq data [18] (Fig. 3A). In the PC3 cells, MLL3 bound in the enhancer region and the promoter region of *PD-L1* (Fig. 3B). The murine transgenic adenocarcinoma of mouse prostate cell line TRAMP-C2 has a high PD-L1 expression and response to PD-L1 antibody treatment in C57BL/6 mice [17]. Depletion of MLL3 with mouse short-hairpin RNAs (shRNAs) decreased the PD-L1 protein expression and RNA levels in TRAMP-C2 cells (Fig. 3C and D). The ChIP assay was used to further explore the histone modification and RNA polymerase II (Pol II) binding. H3K4me1 in the enhancer of PD-L1 was decreased when MLL3 was knocked down TRAMP-C2 cells (Fig. 3E). The phosphorylation of serine 5 in the C-terminus of Pol II activates the gene [19]. Enhancer activation regulates the Pol II-serine 5 phosphorylation (Pol II-S5p). Pol II S-5p was decreased when MLL3 was knocked down in the PC3 and TRAMP-C2 cells (Fig. 3F). We cloned the human promoter and enhancer regions of *PD-L1* separately and together into the PGL3.0 basic plasmid (Fig. 3G). The luciferase assay showed that plasmid with the enhancer of PD-L1 had higher transcription activity than did the plasmid with only the promoter in PC3 cells (Fig. 3H). Furthermore, depletion of MLL3 by shRNAs decreased luciferase activity in cells with transfected with both the promoter and the enhancer of PD-L1 (Fig. 3H). These data indicated that MLL3 regulated PD-L1 at the level of transcription by increasing H3K4 mono-methylation in the enhancer region.

2.4. MLL3 regulated the interaction between enhancer and promoter of PD-L1

Due to MLL3 was located in the enhancer and promoter of *PD-L1*, we further determined the MLL3 effect on interaction between enhancer and promoter of *PD-L1*. Using the Encyclopedia of DNA Elements (ENCODE) database in http://promoter.bx.psu.edu/hi-c/chiapet.php, we analyzed the high-throughput sequencing of Chromosome conformation capture (Hi-C seq) [20] and Virtual circularized chromosome conformation capture (4C)-seq data [21–24] in the *PD-L1* locus. The Hi-C data show that *PD-L1* promoter interacted with the putative enhancer in the 3UTR of *PD-L1* (Fig. 4A). The 4C data show that *PD-L1* promoter interacted with the peaks in the 3UTR of *PD-L1* (Fig. 4B). The interactions between the promoter of *PD-L1* and its putative enhancer were validated by chromosome conformation capture (3C) assays in PC3 cells (Fig. 4C and D). The fusion ligated DNA was sequenced and verified by Sanger sequence (Fig. 4E). These data indicated that the putative enhancer region could interact with promoter of *PD-L1* in PC3 cells.

2.5. MLL3 regulated immune evasion through PD-L1 in mouse

To explore the Mll3/PD-L1 axis in the mice, we generated the Mll3 stable knocking down cell lines. Our studies showed that PD-L1 antibody treatment or Mll3 knocking down significantly inhibited tumor growth compared with mice of the control group (Fig. 5A and B). The Mll3 knocking down the group with PD-L1 antibody treatment had the similar inhibitory level with PD-L1 antibody treatment singly (Fig. 5A and B). These data suggest that Mll3 depletion impaired the mouse

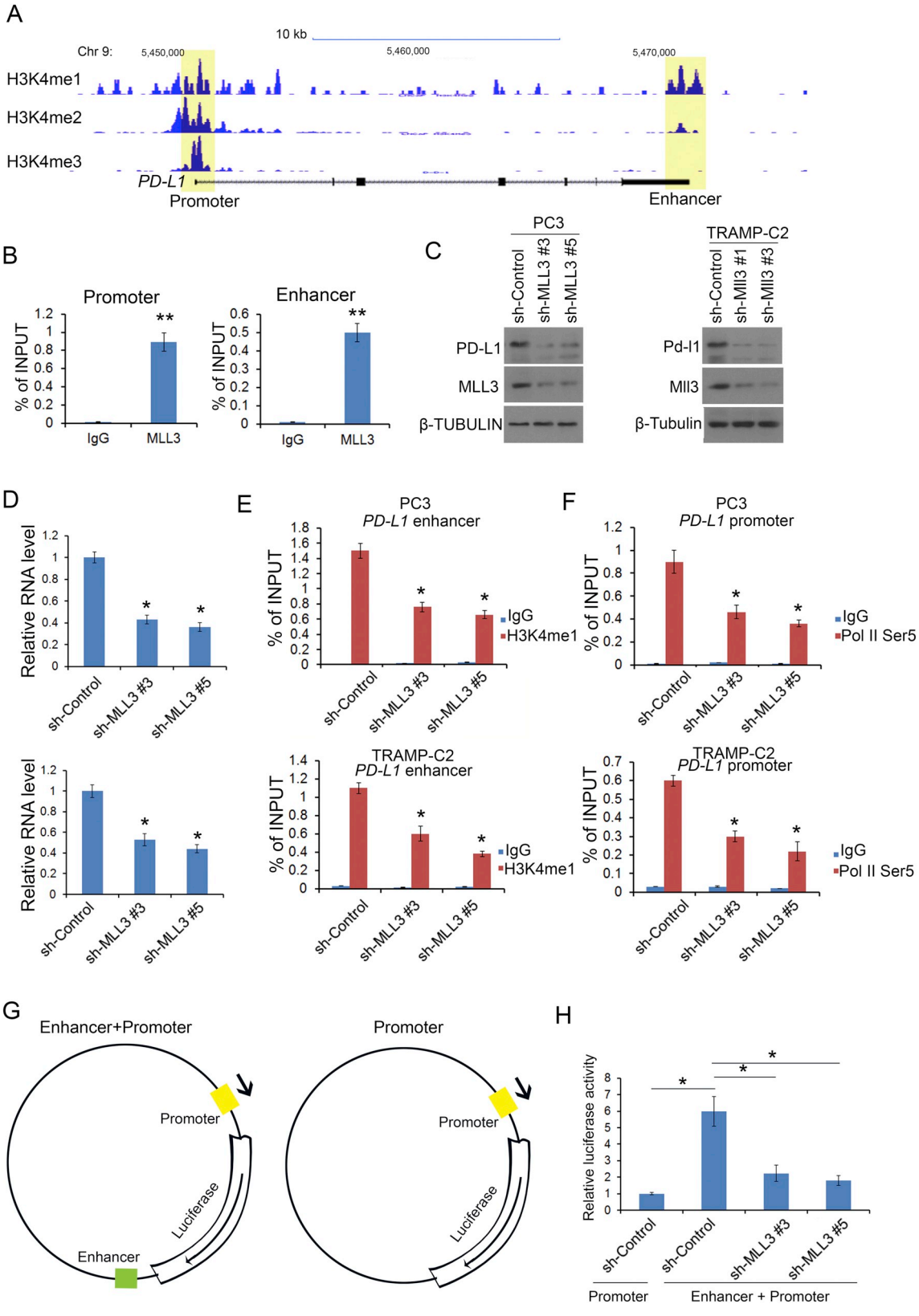

(caption on next page)

Fig. 3. MLL3 regulated PD-L1 transcription through activating enhancer of PD-L1.
(A) Screen shots from the UCSC genome browser showing signal profiles of H3K4me1, H3K4me2 and H3K4me3 in LNCaP.
(B) ChIP-qPCR analysis of MLL3 at the *PD-L1* gene promoter or enhancer in PC3 cells. Immunoprecipitated DNA was detected by real-time PCR. All data shown are mean values ± SD (error bar) from three replicates. $^{**}P < 0.01$.
(C and D) MLL3 regulated protein and RNA level of PD-L1. PC3 or TRAMP-C2 cells were transfected with control (human or mouse) or *MLL3* mRNA-specific shRNAs (human or mouse). 72 h after infection, cells were harvested for WB (C) or RT-qPCR (D). All data are shown as mean values ± SD (n = 3). $^{**}P < 0.01$ comparing to the control group.
(E and F) ChIP-qPCR analysis of H3K4me1 and Pol II Ser-5p at the *PD-L1* gene promoter or enhancer in PC3 cells transfected with control or *MLL3* mRNA-specific shRNAs. Immunoprecipitated DNA was detected by real-time PCR. All data shown are mean values ± SD (error bar) from three replicates. $^{**}P < 0.01$. NS, no significant difference.
(G and H) Left, the schematic diagram showing PD-L1-Luc (promoter + enhancer) and PD-L1-Luc (promoter). Right, measurement of luciferase activity of PD-L1-Luc (promoter + enhancer) and PD-L1-Luc (promoter) in PC3 cells. All data shown are mean values ± SD (error bar) from three replicates. $^{*}P < 0.05$.

xenograft growth and decreased the response to the PD-L1 antibody treatment through PD-L1 downregulation by Mll3 depletion. Moreover, combining Mll3 knocking down and anti-PD-L1 therapy resulted in a similar improvement of overall survival compared to the single-agent treated group (Fig. 5C). As expected from our earlier observations, treatment of tumor-bearing mice with combining Mll3 knocking down and anti-PD-L1 therapy or singly anti-PD-L1 therapy decreased the absolute number of $CD4^+$ and $CD8^+$ T cells (Fig. 5D). To further examine Mll3 and Pd-l1 expression in the xenografts, we re-did the xenografts experiments and collected the protein and RNA samples from xenografts. We found that the tumor volumes were similar size with 40 days after IgG or PD-L1 antibody treatment (Fig. 5E). The Mll3 protein levels were significantly decrease in Mll3 knocking down groups and Pd-l1 protein levels were also significantly decrease in Mll3 knocking down groups (Fig. 5F). The PD-L1 antibody had no increase or decrease effect on Pd-l1 expression in xenografts (Fig. 5F). The RT-PCR data showed the similar RNA levels of *Pd-l1* in the xenografts (Fig. 5G). These data indicated that Mll3 regulated immune evasion through the PD-L1 pathway in mouse.

3. Discussion

Cancer cells utilize the high expression of PD-L1 to escape T-cell-controlled immunosurveillance [14,17]. In prostate cancer, the regulation of PD-L1 still needs to be elucidated. For other regulated manner of PD-L1, CMTM6 could maintain PD-L1 in the endosome and membrane to block its degradation in the lysosome [13,15]. This is the post-transcription regulation for PD-L1. In the transcriptional level, HIF-1α and IRF-1 were identified as the major transcription factors in the promoter of PD-L1 [25,26]. To the best of our knowledge, there is no enhancer for PD-L1 in cancer cells. In this study, we found a novel enhancer region for PD-L1. The enhancer was functional because the H3K4me1 level was related to the *PD-L1* mRNA level. H3K4me1 is the major marker for the enhancer. It is noted that the level of H3K4me1 is related to the activity of enhancer [5]. There are several methyltransferases in the cells. MLL family was a major group for H3K4 methylation in the enhancer region [2]. In the study, we identified that MLL3 was the major mediator of PD-L1 but not other MLLs. MLL2 slightly mediated the PD-L1 expression (Fig. 1). However, the effect was not as robust as MLL3. We also demonstrated that MLL3 bound to the enhancer and promoter of PD-L1. The luciferase assay showed that only promoter had less transcript activity than enhancer plus promoter. The global Hi-C and 4C seq databases demonstrated that the new enhancer had interaction with *PD-L1* promoter in liver tissues, MCF7 and LNCaP cells. Our 3C data also demonstrated that the new enhancer had interaction with *PD-L1* promoter in PC3 cell. Therefore, we defined a new enhancer and a regulator for PD-L1, thus extending the understanding of regulation for immune evasion.

MLL family has served as the oncogene in many cancers [8,27,28]. MLL3 has also usually served as a member of MLL/COMPASS complex in the enhancer region. However, the role of MLL3 in the prostate cancer has been less understood. In the present study, we observed that MLL3 was located in the enhancer of *PD-L1* and regulated the H3K4me1 level in the enhancer. This regulation continuously promoted PD-L1 RNA and protein expression. Furthermore, the expressions of MLL3 and PD-L1 were positively correlated in the clinical prostate cancer tissues in different clinical database. It was noted that both of MLL3 and PD-L1 were highly expressed in metastasis prostate cancer tissues compared to primary prostate cancer tissues. In tumor tolerating model of mice, MLL3 depletion increased the offense of T cell to the tumor in mice. When the T cells were increased, the tumor growths were decreased and survivors of mice were increase. When shRNA control and MLL3 depletion tumors were used anti-PD-L1 treatment, both groups' growths of them were blocked. The RNA and protein levels of PD-L1 were downregulated by MLL3 in xenografts. Therefore, these data demonstrated that MLL3 regulated the tumor evasion from immune through the PD-L1 pathway.

Taken together, these findings enlarged the understanding of the biology regulation of PD-L1 transcription and identified the histone writer MLL3 in the important immune checkpoint. These findings gave prominence to a hidden therapeutic target to conquer immune evasion by tumor cells.

4. Methods and material

4.1. Cell lines, cell culture and transfection

PC-3, TRAMP-C2 and 293T human embryonic kidney cell lines were purchased from ATCC (American Type Culture Collection) (Manassas, USA). PC-3 cells were cultured in RPMI 1640 containing with fetal bovine serum (FBS) (Invitrogen, USA) containing 100 μg/ml penicillin-streptomycin-glutamine (Invitrogen, USA) with 5% CO2 at 37 °C. TRAMP-C2 and 293T cells were maintained in DMEM supplemented with 10% FBS and 100 μg/ml penicillin-streptomycin-glutamine (Invitrogen, USA) at 37 °C with 5% CO_2. Transfections were performed by using Lipofectamine-2000 (Thermo Fisher Scientific).

4.2. Plasmids and antibodies

The pGL3.0-basic and Renella plasmids were purchased from Promega (USA). The MLL3 and MLL4 antibodies were purchased from Novus Biologicals Company (USA). The MLL2 antibodies were purchased from Abcam Company (USA). The human and mouse MLL1 antibodies were purchased from Bethyl Laboratories Company (USA). The human and mouse Tubulin antibodies were purchased from Sigma (USA). The human and mouse PD-L1 antibodies were purchased from Proteintech Company (USA).

4.3. RNA interference

Lentivirus-based control small hairpin RNA and MLL3 gene-specific small hairpin RNAs (shRNAs) were purchased from Sigma-Aldrich as described previously [29]. Viral packaging plasmids (psPAX2 and pVSV-G) and shRNA plasmids were transfected into 293 T cells using Lipofectamine 2000. After 24 h, virus culture medium was discarded and replaced with DMEM supplemented with 10% FBS and 1:100 of

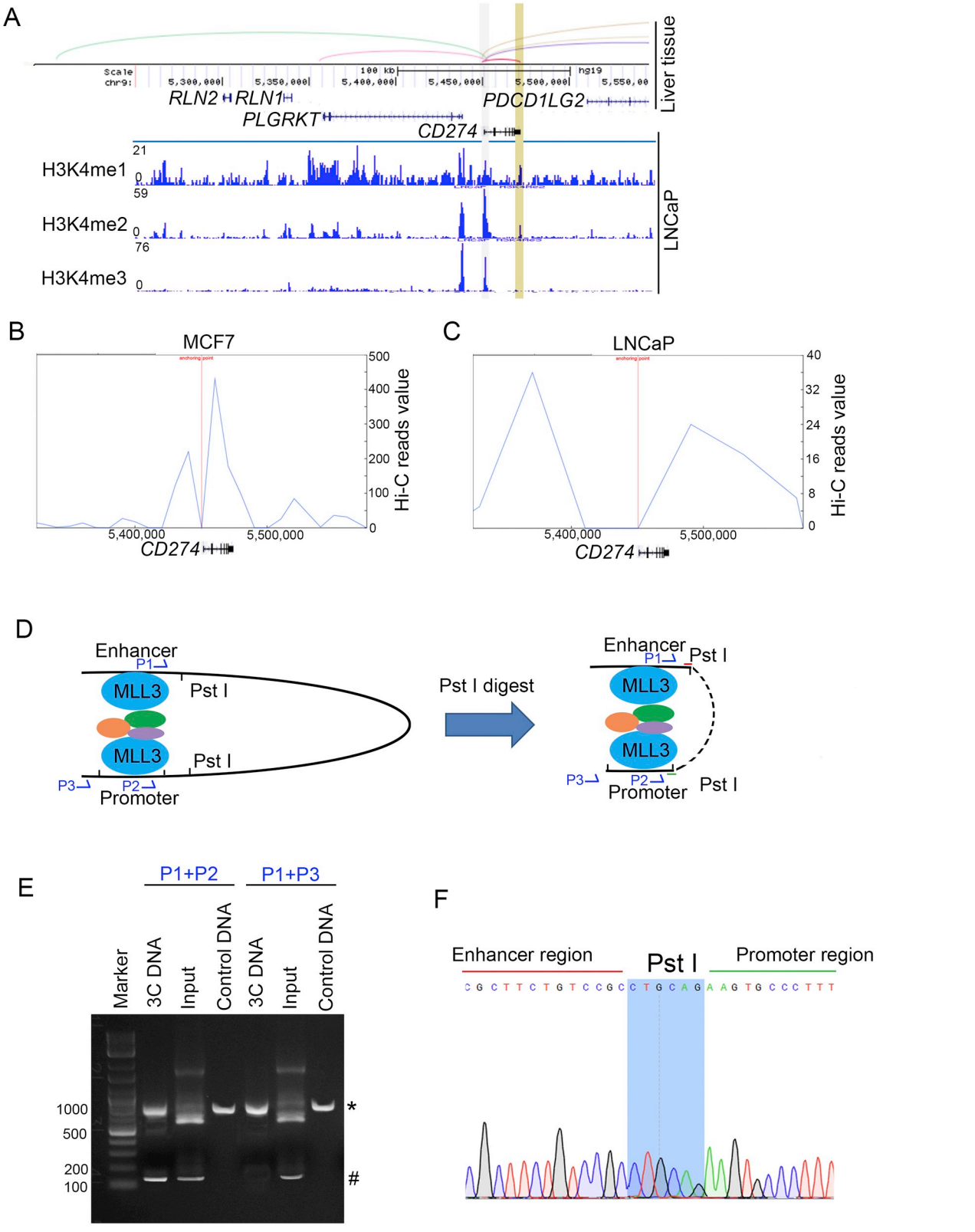

(caption on next page)

Fig. 4. MLL3 regulated PD-L1 transcription through enhancer and promoter interaction.
(A) Screen shots from the UCSC genome browser showing signal profiles of H3K4me1, H3K4me2 and H3K4me3 in LNCaP. Hi-C-seq data from http://promoter.bx.psu.edu/hi-c/chiapet.php showing potential signal binding sites with *CD274* promoter in liver tissues. The gray box is *CD274* promoter region, the yellow box is potential enhancer region.
(B and C) Virtual circularized chromosome conformation capture (4C)-seq data from http://promoter.bx.psu.edu/hi-c/chiapet.php showing potential signal binding regions with *CD274* promoter in MCF7 and LNCaP cells.
(D) The diagram showing that chromosome conformation capture (3C) assay with *Pst* I digesting.
(E and F) Evaluation of the enhancer-promoter interaction at *CD274* target gene loci by chromosome conformation capture (3C) assays (E). *, nonspecific bands; #, ligation bands. The ligation band was sequenced by sanger-sequences, and was shown in (F). Input meant that the genomic DNA was not crossed link with protein, then was digested by Pst I and ligated randomly. Control DNA meant genomic DNA. The red line meant enhancer region; the green line meant promoter region.

sodium Pyruvate. After 48 h transfection, the medium was collected, filtered and added to various cancer cells supplemented with 12 μg/ml of polybrene. Cancer cells were harvested 48 h after puromycin selection.

4.4. Human prostate cancer specimens and RNA isolation from tissues

Hormone-naïve patients with prostate cancer have been treated at the Second Xiangya Hospital (Changsha, China). The primary prostate cancer and castration resistant prostate cancer (CRPC) tissues were freshly and randomly selected from the Second Xiangya Hospital Tissue Registry. This study was approved by the Institutional Review Board of Xiangya Hospital. For the frozen tissues, clinical tissues from patients were acquired from the frozen archives of the Xiangya Hospital with the approval of the Medical Ethics Committee and with noted consent from the Second Xiangya Hospital. Formalin-fixed paraffin-embedded (FFPE) tissues had been harvested and total message RNAs were isolated using a RecoverAll Total Nucleic Acid Isolation Kit (Life Technologies, USA). Isolation of RNAs from FFPE and frozen human prostate cancer tissues was performed as described previously [18,30].

4.5. RNA isolation from cells, reverse transcription PCR (RT-PCR) and real-time qPCR

Total RNA from cells was isolated using TRIzol reagent (Thermo Fisher Scientific, USA). The NanoDrop 2000 spectrophotometer (Bio-Rad, USA) was used to assess RNA yield and quality. RNA was reversely transcribed using Superscript reverse transcriptase kit (Invitrogen, USA) following manufacturer's instructions. The quantitative real-time PCR was performed by mixing cDNA, gene-specific primers and IQ SYRB Green Supermix and detected by QTX iCycler detection system (Bio-Rad). The 2-△Ct method was used. The genes' quantitate fold changes were normalizing to *GAPDH*. The PCR primers for *GAPDH* were forward (F): 5′-AGGTGGAGGAGTGGGTGTCGCTGTT-3′ and reverse (R): 5′-CCGGGAAACTGTGGCGTGATGG-3′; *MLL1,* F: 5′-CACAACTGGGGACATCACAG-3′ and R: 5′-GGTTCACATGCTGAAGCTGA-3′; *MLL2,* F: 5′-CTCTGGATGGGATTGATGCT-3′ and R: 5′-CGTGGCTCTTCCTGTTCTTC-3′; *MLL3,* F: 5′-AAGCAAACGGACTCAGAGGA-3′ and R: 5′-ACAAGCCATAGGAGGTGGTG-3′. *MLL4,* F: 5′-TGTCTATGCGCAGTGGAGAC-3′ and R: 5′-AGTCTGCATCCCCGTATTTG-3′; *PD-L1,* F: 5′-GTACCTTGGCTTTGCCACAT-3′ and R: 5′-CCAACACCACAAGGAGGAGT-3′; mouse *Pd-l1*, F: 5′-GACCAGCTTTTGAAGGGAAATG-3′ and R: 5′-CTGGTTGATTTTGCGGTATGG-3′; mouse 18S, F: 5′-GTAACCCGTTGAACCCCATT-3′ and R: 5′-CCATCCAATCGGTAGTAGCG-3′.

4.6. Western blotting

Cells were harvested and lysed by RIPA buffer on ice, the supernatant was quantified by BCA protein quantification assay (Bio-Rad, USA). Equal amounts of protein sample were added to 4× sample buffer and boiled for 10 min. The sample was subjected to SDS-PAGE analysis and transferred to nitrocellulose membrane. The membrane was blocked by 5% milk for 2 h at room temperature and incubated with primary antibody at 4 °C overnight. The second day, the membrane was washed three times with 1 × TBST and incubated with horseradish peroxidase-conjugated secondary antibodies for 1 h at room temperature. The protein bands were visualized by super signal West Pico Stable Peroxide Solution (Thermo Fisher Scientific, USA).

4.7. Chromatin immunoprecipitation (ChIP) assay

ChIP was performed as described previously [18,31]. The cell lysate was sonicated and subjected to immunoprecipitation using anti-MLL3, Pol II Ser5p or H3K4me1 antibody or nonspecific IgG. After extensive wash, immunoprecipitated DNA was amplified by real-time PCR. The ChIP primers for *PD-L1 promoter* were forward (F): 5′-CAAGGTGCGTTCAGATGTTG-3′ and reverse (R):5′-TCCTGACCTTCGGTGAAATC-3′; *PD-L1 enhancer* were forward (F): 5′-ACTCCTCCTTGTGGTGTTGG-3′ and reverse (R): 5′-AAGAAAATGGACATGCTGGTG-3′.

4.8. Quantitative chromosome conformation capture (3C) assay

3C assays were performed as described previously [32]. Briefly, the crosslinked chromatin was digested with specific restriction enzymes *Pst* I overnight. The crosslinking was reversed and ligated DNA was purified. Primers for qPCR are listed: Primer 1 (P1) 5′-CACTGAGACTCTCAGTCATGCAG-3′; P2 5′-CAGTTCTGCGCAGCTTCCC-3′; P3 5′-CATAACCAATGCAAGGGCTATC-3′.

4.9. Generation and treatment of TRAMP-C2 xenografts in mice

6-week-old Balb/c mice (Nanjing University) were used for animal experiments. And the animal study was approved by the IACUC at Xiangya Hospital. All mice were in standard conditions house with a 12 h light/dark cycle and access to food and water ad libitum. TRAMP-C2 cells (1×10^7 in 100 μl 1 × PBS plus 100 μl Matrigel (BD Biosciences, USA)) were injected s.c. into the right flank of mice. The volume of xenografts was measured every other day and calculated using the formula $L \times W^2 \times 0.5$. After xenografts reached a size of approximately 100 mm^3, mice carrying the similar type of tumors were randomized into different groups and anti-PD-L1 (200 μg, i.p., given at days 0, 3, 6, and 9). Mice were euthanized and tumors collected from all animals once tumors reached a volume of 500 mm^3. TRAMP-C2 cells were transfected with control (mouse) or *Mll3* mRNA-specific shRNAs (mouse). 40 days after injection, xenografts were harvested by dry ice frozen and homogenization. Half xenografts scraps were in the RIPA lysis buffer for Western blot. Half xenografts scraps were in the TRIZOL buffer for RT-PCR assay.

4.10. Flow cytometry analysis

For flow cytometry analysis of mouse tissue samples, tumors were cut into small pieces and digested with 2 mg/ml collagenase (Sigma, USA) in DMEM for 1 h at 37 °C. Cells were filtered through 70 μm nylon strainer and re-suspended in red blood cell lysis buffer (Biolegend, USA) for 3 min at room temperature. Cells were then suspended in PBS with 2% BSA and co-stained with the following antibodies: CD4 (Biolegend, 100510, FITC conjugated) and CD8 (Biolegend,100708, PE conjugated). After incubated with antibody for 30 min, cells were washed with PBS and analyzed on the flow cytometer.

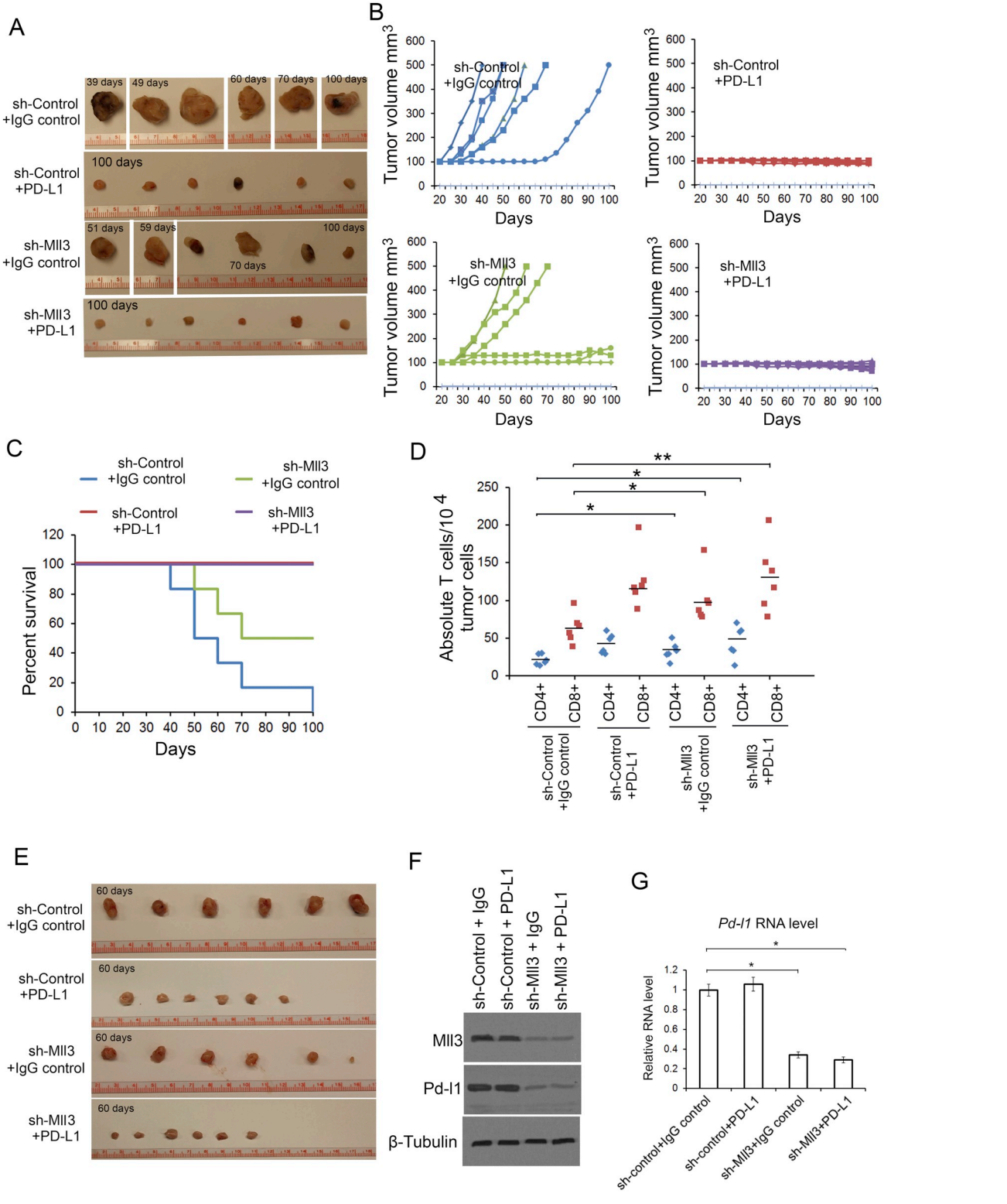

(caption on next page)

Fig. 5. MLL3 regulated PD-L1 and promoted cancer immunity.
(A and B) TRAMP-C2 mouse prostate cancer cells were transduced with lentivirus for empty vector (EV) or the MLL3 shRNAs mix. 72 h after puromycin selection, 5×10^6 control or MLL3 knocking down cells were injected subcutaneously into Balb/c mice. Mice (n = 6/group) were treated with anti-PD-L1 (200 μg) or non-specific IgG for 80 days. The day of harvesting the tumor was shown in each tumor. The tumors were not harvest in the same day. Growth curves of tumors with different treatments are shown in (B).
(C) At the end of treatment, the numbers of survival mouse were count. The survival curves were shown in (C).
(D) At the end of treatment, the numbers of infiltrated CD8 + T cells and CD4 + T cells in tumors with different treatments were analyzed by FACS. All data are shown as mean values ± SD (n = 8). $^*P < 0.05$.
(E) TRAMP-C2 mouse prostate cancer cells were transduced with lentivirus for empty vector (EV) or the MLL3 shRNAs mix. 72 h after puromycin selection, 5×10^6 control or MLL3 knocking down cells were injected subcutaneously into Balb/c mice. Mice (n = 6/group) were treated with anti-PD-L1 (200 μg) or non-specific IgG for 40 days. The day of harvesting the tumor was shown in each tumor. The tumors were harvest in the same day (60 days).
(F and G) MLL3 regulated protein and RNA level of PD-L1 in xenografts. TRAMP-C2 cells were transfected with control (mouse) or *Mll3* mRNA-specific shRNAs (mouse). 60 days after injection, xenografts were harvested for WB (F) or RT-qPCR (G) by dry ice frozen and homogenization. All data are shown as mean values ± SD (n = 3). $^*P < 0.05$ comparing to the control group.

5. Statistical analysis

Experiments in the paper were carried out with three replicates. Statistical analyses were performed using Student's *t*-test for most comparisons. The $P < 0.05$ is statistically significance.

Conflict of interest

The authors declare no conflict of interest.

Acknowledgments

The research was supported by basic research Foundation from the Second Xiangya Hospital and Fellowship from Second Xiangya Hospital and Central South University.

Author contribution

Wei Xiong, Huanghao Deng and Changkun Huang performed the experiments and wrote the paper, Chong Zeng, Chengzhu Jian, Zhaohui Zhong and Xiaokun Zhao collected and performed clinical data, Liang Zhu wrote the paper and convinces the data.

Appendix A. Supplementary data

Supplementary data to this article can be found online at https://doi.org/10.1016/j.bbadis.2018.10.027.

References

[1] S. Heinz, C.E. Romanoski, C. Benner, C.K. Glass, The selection and function of cell type-specific enhancers, Nat. Rev. Mol. Cell Biol. 16 (2015) 144–154.
[2] K.M. Dorighi, T. Swigut, T. Henriques, N.V. Bhanu, B.S. Scruggs, N. Nady, C.D. Still 2nd, B.A. Garcia, K. Adelman, J. Wysocka, Mll3 and Mll4 facilitate enhancer RNA synthesis and transcription from promoters independently of H3K4 monomethylation, Mol. Cell 66 (2017) 568–576 e564.
[3] S. Ghisletti, I. Barozzi, F. Mietton, S. Polletti, F. De Santa, E. Venturini, L. Gregory, L. Lonie, A. Chew, C.L. Wei, J. Ragoussis, G. Natoli, Identification and characterization of enhancers controlling the inflammatory gene expression program in macrophages, Immunity 32 (2010) 317–328.
[4] M.P. Creyghton, A.W. Cheng, G.G. Welstead, T. Kooistra, B.W. Carey, E.J. Steine, J. Hanna, M.A. Lodato, G.M. Frampton, P.A. Sharp, L.A. Boyer, R.A. Young, R. Jaenisch, Histone H3K27ac separates active from poised enhancers and predicts developmental state, Proc. Natl. Acad. Sci. U. S. A. 107 (2010) 21931–21936.
[5] N.D. Heintzman, G.C. Hon, R.D. Hawkins, P. Kheradpour, A. Stark, L.F. Harp, Z. Ye, L.K. Lee, R.K. Stuart, C.W. Ching, K.A. Ching, J.E. Antosiewicz-Bourget, H. Liu, X. Zhang, R.D. Green, V.V. Lobanenkov, R. Stewart, J.A. Thomson, G.E. Crawford, M. Kellis, B. Ren, Histone modifications at human enhancers reflect global cell-type-specific gene expression, Nature 459 (2009) 108–112.
[6] R.C. Rao, Y. Dou, Hijacked in cancer: the KMT2 (MLL) family of methyltransferases, Nat. Rev. Cancer 15 (2015) 334–346.
[7] M. Merika, A.J. Williams, G. Chen, T. Collins, D. Thanos, Recruitment of CBP/p300 by the IFN beta enhanceosome is required for synergistic activation of transcription, Mol. Cell 1 (1998) 277–287.
[8] D. Hu, X. Gao, M.A. Morgan, H.M. Herz, E.R. Smith, A. Shilatifard, The MLL3/MLL4 branches of the COMPASS family function as major histone H3K4 monomethylases at enhancers, Mol. Cell. Biol. 33 (2013) 4745–4754.
[9] L. Chen, X. Han, Anti-PD-1/PD-L1 therapy of human cancer: past, present, and future, J. Clin. Invest. 125 (2015) 3384–3391.
[10] R.S. Dronca, X. Liu, S.M. Harrington, L. Chen, S. Cao, L.A. Kottschade, R.R. McWilliams, M.S. Block, W.K. Nevala, M.A. Thompson, A.S. Mansfield, S.S. Park, S.N. Markovic, H. Dong, T cell Bim levels reflect responses to anti-PD-1 cancer therapy, JCI Insight 1 (2016).
[11] L. Shi, S. Chen, L. Yang, Y. Li, The role of PD-1 and PD-L1 in T-cell immune suppression in patients with hematological malignancies, J. Hematol. Oncol. 6 (2013) 74.
[12] L.V. Riella, A.M. Paterson, A.H. Sharpe, A. Chandraker, Role of the PD-1 pathway in the immune response, Am. J. Transplant. 12 (2012) 2575–2587.
[13] M.L. Burr, C.E. Sparbier, Y.C. Chan, J.C. Williamson, K. Woods, P.A. Beavis, E.Y.N. Lam, M.A. Henderson, C.C. Bell, S. Stolzenburg, O. Gilan, S. Bloor, T. Noori, D.W. Morgens, M.C. Bassik, P.J. Neeson, A. Behren, P.K. Darcy, S.J. Dawson, I. Voskoboinik, J.A. Trapani, J. Cebon, P.J. Lehner, M.A. Dawson, CMTM6 maintains the expression of PD-L1 and regulates anti-tumour immunity, Nature 549 (2017) 101–105.
[14] J. Zhang, X. Bu, H. Wang, Y. Zhu, Y. Geng, N.T. Nihira, Y. Tan, Y. Ci, F. Wu, X. Dai, J. Guo, Y.H. Huang, C. Fan, S. Ren, Y. Sun, G.J. Freeman, P. Sicinski, W. Wei, Cyclin D-CDK4 kinase destabilizes PD-L1 via cullin 3-SPOP to control cancer immune surveillance, Nature 553 (2018) 91–95.
[15] R. Mezzadra, C. Sun, L.T. Jae, R. Gomez-Eerland, E. de Vries, W. Wu, M.E.W. Logtenberg, M. Slagter, E.A. Rozeman, I. Hofland, A. Broeks, H.M. Horlings, L.F.A. Wessels, C.U. Blank, Y. Xiao, A.J.R. Heck, J. Borst, T.R. Brummelkamp, T.N.M. Schumacher, Identification of CMTM6 and CMTM4 as PD-L1 protein regulators, Nature 549 (2017) 106–110.
[16] A.J. Ligocki, J.Y. Niederkorn, Advances on non-CD4 + Foxp3 + T regulatory cells: CD8 +, type 1, and double negative T regulatory cells in organ transplantation, Transplantation 99 (2015) 1553–1559.
[17] P. Yu, J.C. Steel, M. Zhang, J.C. Morris, R. Waitz, M. Fasso, J.P. Allison, T.A. Waldmann, Simultaneous inhibition of two regulatory T-cell subsets enhanced Interleukin-15 efficacy in a prostate tumor model, Proc. Natl. Acad. Sci. U. S. A. 109 (2012) 6187–6192.
[18] Y. Zhao, L. Wang, S. Ren, P.R. Blackburn, M.S. McNulty, X. Gao, M. Qiao, R.L. Vessella, M. Kohli, J. Zhang, R.J. Karnes, D.J. Tindall, Y. Kim, R. MacLeod, S.C. Ekker, T. Kang, Y. Sun, H. Huang, Activation of P-TEFb by androgen receptor-regulated enhancer RNAs in castration-resistant prostate cancer, Cell Rep. 15 (2016) 599–610.
[19] S.H. Ahn, M. Kim, S. Buratowski, Phosphorylation of serine 2 within the RNA polymerase II C-terminal domain couples transcription and 3′ end processing, Mol. Cell 13 (2004) 67–76.
[20] J.H. Im, S.M. Yoon, H.C. Park, J.H. Kim, J.I. Yu, T.H. Kim, J.W. Kim, T.K. Nam, K. Kim, H.S. Jang, J.H. Kim, M.S. Kim, W.S. Yoon, I. Jung, J. Seong, Radiotherapeutic strategies for hepatocellular carcinoma with portal vein tumour thrombosis in a hepatitis B endemic area, Liver Int. 37 (2017) 90–100.
[21] S.S. Rao, M.H. Huntley, N.C. Durand, E.K. Stamenova, I.D. Bochkov, J.T. Robinson, A.L. Sanborn, I. Machol, A.D. Omer, E.S. Lander, E.L. Aiden, A 3D map of the human genome at kilobase resolution reveals principles of chromatin looping, Cell 159 (2014) 1665–1680.
[22] B. Mifsud, F. Tavares-Cadete, A.N. Young, R. Sugar, S. Schoenfelder, L. Ferreira, S.W. Wingett, S. Andrews, W. Grey, P.A. Ewels, B. Herman, S. Happe, A. Higgs, E. LeProust, G.A. Follows, P. Fraser, N.M. Luscombe, C.S. Osborne, Mapping long-range promoter contacts in human cells with high-resolution capture Hi-C, Nat. Genet. 47 (2015) 598–606.
[23] A.J. Rubin, B.C. Barajas, M. Furlan-Magaril, V. Lopez-Pajares, M.R. Mumbach, I. Howard, D.S. Kim, L.D. Boxer, J. Cairns, M. Spivakov, S.W. Wingett, M. Shi, Z. Zhao, W.J. Greenleaf, A. Kundaje, M. Snyder, H.Y. Chang, P. Fraser, P.A. Khavari, Lineage-specific dynamic and pre-established enhancer-promoter contacts cooperate in terminal differentiation, Nat. Genet. 49 (2017) 1522–1528.
[24] I. Chepelev, G. Wei, D. Wangsa, Q. Tang, K. Zhao, Characterization of genome-wide enhancer-promoter interactions reveals co-expression of interacting genes and modes of higher order chromatin organization, Cell Res. 22 (2012) 490–503.
[25] A. Garcia-Diaz, D.S. Shin, B.H. Moreno, J. Saco, H. Escuin-Ordinas, G.A. Rodriguez, J.M. Zaretsky, L. Sun, W. Hugo, X. Wang, G. Parisi, C.P. Saus, D.Y. Torrejon, T.G. Graeber, B. Comin-Anduix, S. Hu-Lieskovan, R. Damoiseaux, R.S. Lo, A. Ribas, Interferon receptor signaling pathways regulating PD-L1 and PD-L2 expression, Cell Rep. 19 (2017) 1189–1201.

[26] J.M. Chinai, M. Janakiram, F. Chen, W. Chen, M. Kaplan, X. Zang, New immunotherapies targeting the PD-1 pathway, Trends Pharmacol. Sci. 36 (2015) 587–595.
[27] S. Weirich, S. Kudithipudi, I. Kycia, A. Jeltsch, Somatic cancer mutations in the MLL3-SET domain alter the catalytic properties of the enzyme, Clin. Epigenetics 7 (2015) 36.
[28] J. Zhu, M.A. Sammons, G. Donahue, Z. Dou, M. Vedadi, M. Getlik, D. Barsyte-Lovejoy, R. Al-awar, B.W. Katona, A. Shilatifard, J. Huang, X. Hua, C.H. Arrowsmith, S.L. Berger, Gain-of-function p53 mutants co-opt chromatin pathways to drive cancer growth, Nature 525 (2015) 206–211.
[29] J. Zhao, Y. Zhao, L. Wang, J. Zhang, R.J. Karnes, M. Kohli, G. Wang, H. Huang, Alterations of androgen receptor-regulated enhancer RNAs (eRNAs) contribute to enzalutamide resistance in castration-resistant prostate cancer, Oncotarget 7 (2016) 38551–38565.
[30] L. Tang, F. Wei, Y. Wu, Y. He, L. Shi, F. Xiong, Z. Gong, C. Guo, X. Li, H. Deng, K. Cao, M. Zhou, B. Xiang, X. Li, Y. Li, G. Li, W. Xiong, Z. Zeng, Role of metabolism in cancer cell radioresistance and radiosensitization methods, J. Exp. Clin. Cancer Res. 37 (2018) 87.
[31] P. Zhang, D. Wang, Y. Zhao, S. Ren, K. Gao, Z. Ye, S. Wang, C.W. Pan, Y. Zhu, Y. Yan, Y. Yang, D. Wu, Y. He, J. Zhang, D. Lu, X. Liu, L. Yu, S. Zhao, Y. Li, D. Lin, Y. Wang, L. Wang, Y. Chen, Y. Sun, C. Wang, H. Huang, Intrinsic BET inhibitor resistance in SPOP-mutated prostate cancer is mediated by BET protein stabilization and AKT-mTORC1 activation, Nat. Med. 23 (2017) 1055–1062.
[32] H. Hagege, P. Klous, C. Braem, E. Splinter, J. Dekker, G. Cathala, W. de Laat, T. Forne, Quantitative analysis of chromosome conformation capture assays (3C-qPCR), Nat. Protoc. 2 (2007) 1722–1733.